JOURNAL OF MOLECULAR SPECTROSCOPY **175,** 277–288 (1996)
ARTICLE NO. 0033

Infrared Spectroscopy of the Amidogen Ion, NH_2^+

Y. Kabbadj,[1] T. R. Huet,[2] D. Uy, and T. Oka

Department of Chemistry and Department of Astronomy and Astrophysics, The University of Chicago, Chicago, Illinois 60637

Received May 5, 1995; in revised form November 20, 1995

The absorption spectrum of NH_2^+ has been recorded continuously between 3500 and 2900 cm^{-1} with a difference frequency laser spectrometer along with the velocity modulation technique. The molecular ions were produced in the positive column of an ac glow discharge with a gas mixture of $N_2/H_2/He$ in a ratio of around 1/1/100 with a total pressure of ~7 Torr. In view of the very low barrier to linearity (155 cm^{-1}) and the high bending vibrational states involved, the observed spectrum was analyzed using the Hamiltonian for linear molecules. The choice of this model is discussed in relation to the previous experimental results and *ab initio* calculations. Four hot bands have been assigned: $2\nu_2^0 + \nu_3 \leftarrow 2\nu_2^0$, $\nu_1 + \nu_3 \leftarrow \nu_1$, $\nu_1 + \nu_2 + \nu_3 \leftarrow \nu_1 + \nu_2$, and $2\nu_1 + \nu_3 \leftarrow 2\nu_1$. The matrix elements of the Hamiltonian used for the analysis of the rotational fine structure of the excited degenerate bending vibrational states of a linear molecule in a triplet electronic state are presented. The resultant rotational and vibrational constants are discussed.

I. INTRODUCTION

The amidogen ion, NH_2^+, is one of the most fundamental molecular ions which exist abundantly in laboratory plasmas containing hydrogen and nitrogen. It is also expected to play an important role in the plasma chemistry of both dense (*1, 2*) and diffuse (*3*) interstellar molecular clouds. Because of the simplicity of its structure which is isoelectronic to CH_2, there have been many *ab initio* theoretical studies on NH_2^+. A qualitative argument using Walsh's diagram (*4*) indicates that both CH_2 and NH_2^+ have closely separated singlet and triplet electronic states in which the molecules are bent and nearly linear, respectively. Lee and Morokuma (*5*) were the first to conduct an *ab initio* SCF-CI calculation on both the triplet and the singlet states of NH_2^+ and showed that the $^3B_1$ triplet state is lower in energy and thus constitutes the ground state as in CH_2. They also showed that NH_2^+ in the triplet state is more quasilinear than CH_2, having a larger bond angle (146° vs 138°) and a lower barrier to linearity (560 cm^{-1} vs 1680 cm^{-1}). Subsequently, more complete *ab initio* calculations predicted progressively higher quasilinearity for the NH_2^+ triplet state, the subject of this paper. Thus Peyerimhoff and Buenker (*6*) reported 149.6° and 330 cm^{-1} and Jensen *et al.* (*7*) reported 153.2° and 209 cm^{-1}. In the recent extensive treatment into which our experimental results are incorporated, Barclay *et al.* (*8*) reported the bond angle of 153.8° and the barrier height to linearity as low as 155 cm^{-1}. Clearly the barrier is below the zero-point energy level of the ν_2 bending vibration, and the molecule can be regarded as practically linear, although the presence of the potential hump will affect the rotation–vibration levels. For this reason, we use the vibration–rotation quantum numbers for linear molecules v, ℓ, and N to describe the energy levels of NH_2^+ in this paper.

By now, it is well-established by *ab initio* calculations and experiments that although the structures and the potential surfaces of CH_2 and NH_2^+ are qualitatively similar, they are quite different quantitatively. Potential curves for the bending angles of CH_2 and NH_2^+ are shown in Fig. 1. For CH_2, the potential curves reported by Duxbury and Jungen (*9*) and Alijah and Duxbury (*10*) are used. For NH_2^+, the potential reported by Barklay *et al.* (*8*) for the triplet state and the theoretical potential reported by Peric *et al.* (*11*) for the singlet state are used. Vibrational frequencies of NH_2^+ in the triplet ground state had been predicted by DeFrees and McLean (*12*) and by Jensen *et al.* (*7*); their predicted values for ν_3 of 3308 and 3344 cm^{-1}, respectively, turned out to be in good agreement with the experimental value (*13*) of 3359.932 cm^{-1}. Jensen *et al.* (*7*), Barclay *et al.* (*8*), and Chambaud *et al.* (*14*) have given extensive calculations on the intramolecular dynamics of NH_2^+ to determine vibration–rotation energy levels. They are very useful for future experiments, especially the intensity information given by Chambaud *et al.* (*14*).

While there have been a vast number of experimental studies on the quantum mechanics of CH_2 (see reviews by Bunker (*15*) and Schaefer (*16*) and other references quoted by Barclay *et al.* (*8*)) since the 1959 discovery of its spectrum by Herzberg and Shoosmith (*17*), spectroscopic studies of

[1] Present address: Laboratoire de Physico-Chimie de l'Atmosphère, Université du Littoral, Quai Freycinet 1, B.P. 5526, 59379 Dunkerque Cédex 1, France.

[2] Present address: Laboratoire de Spectroscopie Hertzienne, Université de Lille I, 59655 Villeneuve d'Ascq, France.

0022-2852/96 $18.00

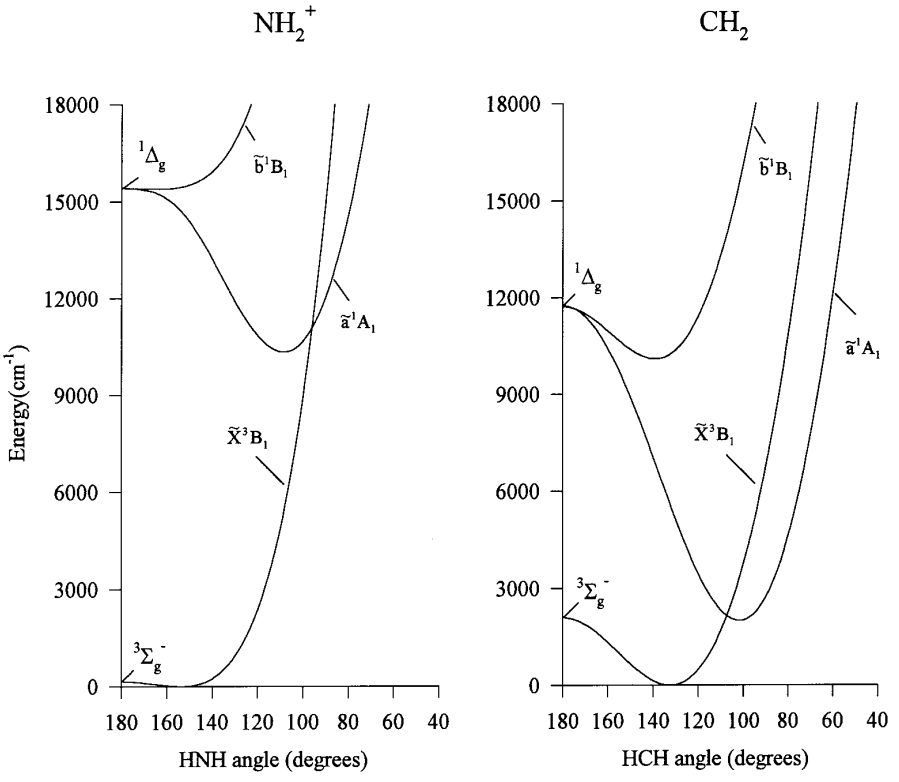

FIG. 1. The bending potential energy curves of the lowest-lying electronic states of NH_2^+ and CH_2 calculated from the data of the literature (see text).

NH_2^+ are very limited so far. Dunlavey *et al.* (*18*) observed the photoelectron spectrum of NH_2^+ and determined the separation between the $^3B_1$ state and the $^1A_1$ state of NH_2^+ to be 0.99 ± 0.02 eV and the bending frequency $\nu_2 = 840 \pm 50$ cm^{-1}. Herzberg observed spectra in the region 2200–2400 Å, which he ''considered as strong candidates for NH_3^+ and NH_2^+'' (*19*), but their identification is yet to be confirmed. Gibson *et al.* (*20*) studied the photoionization of NH_2^+ and determined the separation between the triplet and the singlet state of NH_2^+ to be 1.30 ± 0.01 eV, considerably higher than that given by Dunlavey *et al.* (*18*). The ionization potentials of NH_2^+ were also revised. Subsequent *ab initio* studies have given theoretical values that agree with those experimental values. Reference (*8*) gives $\nu_2 = 845$ cm^{-1} and Ref. (*7*) gives the singlet–triplet splitting as 1.299 eV.

So far, the only direct spectroscopic study of NH_2^+ has been our observation of the high-resolution infrared spectrum of the ν_3 fundamental band corresponding to the antisymmetric N–H stretching vibration (*13*). Fifty-three rovibrational transitions with triplet structure were assigned, and accurate rotation–vibration constants and magnetic fine structure constants were determined. More recently, we have conducted further spectroscopy of positive column discharges using N_2/H_2/He gas mixtures and have obtained extremely rich spectra of $N_xH_y^+$ molecular ions. We have assigned in this thicket of spectral lines 32 new hot bands of HN_2^+ reaching the $v_1v_2^\ell v_3 = 11^13$ vibrational state, 10 613 cm^{-1} above the ground state (*21*). The spectrum demonstrated extremely high vibrational temperatures of 4000, 1550, and 3100 K for the ν_1, ν_2, and ν_3 vibrations, respectively. We also assigned the $\nu_2 + \nu_3 \leftarrow \nu_2$ hot band of NH_3^+ (*22*) in the same spectral range.

In this paper, we report our observation and analysis of four NH_2^+ hot bands: $2\nu_2^0 + \nu_3 \leftarrow 2\nu_2^0$, $\nu_1 + \nu_3 \leftarrow \nu_1$, $\nu_1 + \nu_2 + \nu_3 \leftarrow \nu_1 + \nu_2$, and $2\nu_1 + \nu_3 \leftarrow 2\nu_1$. These data, as well as our earlier results by Okumura *et al.* (*13*), are analyzed. For the extreme quasilinearity mentioned above, we use rovibrational quantum numbers for a linear molecule instead of the asymmetric rotor quantum numbers of Ref. (*13*). Thus, the $K_a = 0$ series and $K_a = 1$ series of the fundamental band in Ref. (*13*) are the $\nu_3 \leftarrow 0$ fundamental band and the $\nu_2^1 + \nu_3 \leftarrow \nu_2^1$ hot band, respectively, in the present nomenclature (*23*). The spin–spin and the spin–rotation matrix elements in this nomenclature are derived based on the classic paper by Van Vleck (*24*) and used in this analysis.

II. EXPERIMENTAL DETAILS

Spectra were recorded during our general study of a N_2/H_2/He glow discharge (*21, 22*). The details of the experi-

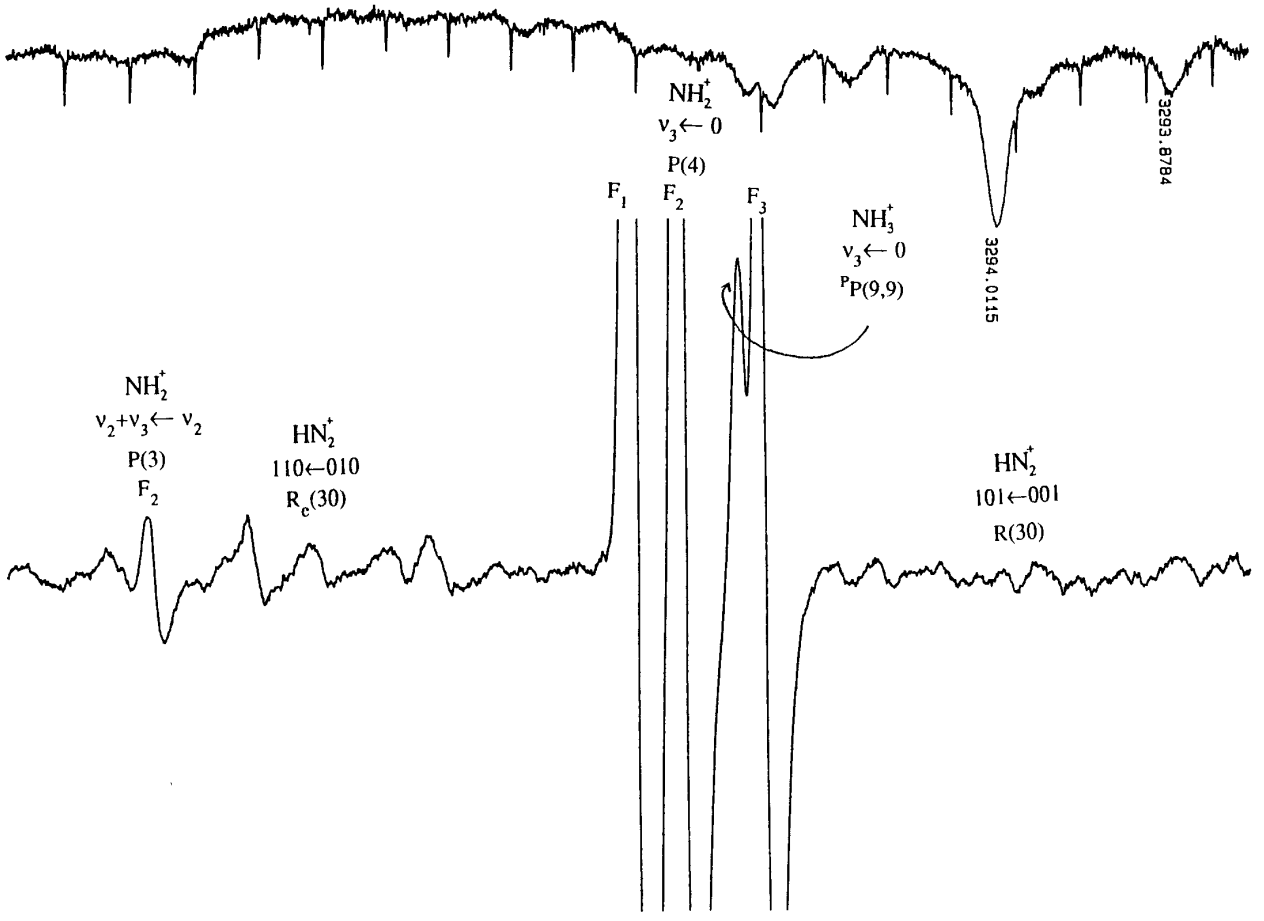

FIG. 2. Example of the spectrum recorded in an N_2/H_2/He discharge. The upper trace shows two C_2H_4 reference lines.

mental part were given in these papers, and are briefly described below.

We used a difference frequency laser spectrometer assembled by Crofton *et al.* (*25*) following the original design of Pine (*26*). The counterpropagating multiple beam technique due to Bawendi *et al.* (*27*) for the noise subtraction, and the velocity modulation method introduced by Gudeman *et al.* (*28*) for the detection of the molecular ion signals were used. Wavenumber calibration was made against NH_3 and C_2H_4 lines measured by Johns (*29*) and Pine (*30*), respectively. Spectra were recorded continuously between 3500 and 2900 cm^{-1}, using a water-cooled glass discharge cell or a liquid-nitrogen-cooled one. In the regions between 3500 and 3225 cm^{-1}, and between 3075 and 2900 cm^{-1}, we used a water-cooled glass discharge cell with a gas mixture of 40 mTorr N_2, 40 mTorr H_2, and 7 Torr He. For the spectra obtained between 3225 and 3075 cm^{-1}, we used a liquid-nitrogen-cooled glass discharge cell with a gas mixture of 60 mTorr N_2, 60 mTorr H_2, and 7 Torr He.

An example of the observed spectrum is shown in Fig. 2. The chemistry was optimized with the aim of obtaining strong NH_2^+ signals. However, intense lines of the NH_2^+ (*21*) and NH_3^+ (*22*) spectra were also observed including their hot bands. We believe that these observations were possible for two reasons. First, the chemistry used produced abundant molecular ions in excited vibrational states, and second, high sensitivity may be reached with our system.

III. RESULTS

As we mentioned before, we consider NH_2^+ as linear in its ground electronic state, with symmetry $^3\Sigma_g^-$. Therefore, the vibrational levels are represented by the symbol (v_1, $v_2^{\ell_2}$, v_3). In this notation, v_1, v_2, and v_3 denote the numbers of vibrational quanta in the ν_1 vibrational mode (N–H symmetric stretching), the ν_2 vibrational mode (H–N–H bending), and the ν_3 vibrational mode (N–H antisymmetric stretching), respectively, and ℓ_2 is the quantum number associated with the vibrational angular momentum corresponding to the doubly degenerate ν_2 vibration. Note that the definition of ν_2 differs between the linear model adopted in this paper and the bent model used in earlier literature. Johns' correlation

TABLE 1a
The Hamiltonian Matrix Elements for NH_2^+ Considered as Linear: The Bending Number of Vibrational Quantum $\upsilon_2 = 0$

$$(1,1)_{F_3} = E_v + B_v(J+1)(J+2) - D_v(J+1)^2(J+2)^2 - (a-a_0)(J+2) - \alpha\,\frac{J+2}{2J+1}$$

$$(2,2)_{F_2} = E_v + B_vJ(J+1) - D_vJ^2(J+1)^2 - (a-a_0) + \alpha$$

$$(3,3)_{F_1} = E_v + B_vJ(J-1) - D_vJ^2(J-1)^2 + (a-a_0)(J-1) - \alpha\,\frac{J-1}{2J+1}$$

$$(1,2) = 0$$

$$(1,3) = 3\alpha\frac{\sqrt{J(J+1)}}{2J+1}$$

$$(2,3) = 0$$

TABLE 1b
The Hamiltonian Matrix Elements for NH_2^+ Considered as Linear: The Bending Number of Vibrational Quantum $\upsilon_2 = 1$

$$(1,1)^1_{F_3} = E_v + B_v\left[(J+1)(J+2)-1\right] - D_v\left[(J+1)(J+2)-1\right]^2 - (J+2)\left[(a-a_0) - \frac{3a}{(J+1)(J+2)}\right] - \alpha\,\frac{J+2}{2J+1}\left[1 - \frac{3}{(J+1)(J+2)}\right] + g_{22}$$

$$(2,2)^1_{F_2} = E_v + B_v\left[J(J+1)-1\right] - D_v\left[J(J+1)-1\right]^2 - \left[(a-a_0) - \frac{3a}{J(J+1)}\right] + \alpha\left[1 - \frac{3}{J(J+1)}\right] + g_{22}$$

$$(3,3)^1_{F_1} = E_v + B_v\left[J(J-1)-1\right] - D_v\left[J(J-1)-1\right]^2 + (J-1)\left[(a-a_0) - \frac{3a}{J(J-1)}\right] - \alpha\,\frac{J-1}{2J+1}\left[1 - \frac{3}{J(J-1)}\right] + g_{22}$$

$$(4,4)^{-1}_{F_3} = (1,1)^1_{F_3}\ ;\ (5,5)^{-1}_{F_2} = (2,2)^1_{F_2}\ ;\ (6,6)^{-1}_{F_1} = (3,3)^1_{F_1}$$

$$(1,2) = -\frac{3}{J+1}\sqrt{\frac{J+2}{2J+1}}(aJ + \alpha)$$

$$(1,3) = 3\alpha\frac{\sqrt{(J-1)(J+2)}}{2J+1}$$

$$(1,4) = \frac{1}{2}q(J+1)(J+2)$$

$$(1,5) = \frac{1}{2}\sqrt{\frac{J+2}{2J+1}}(bJ + \beta)$$

$$(1,6) = \frac{1}{2}\beta\frac{\sqrt{(J-1)(J+2)}}{2J+1}$$

$$(2,3) = -\frac{3}{J}\sqrt{\frac{J-1}{2J+1}}(a(J+1) - \alpha)$$

$$(2,5) = \frac{1}{2}qJ(J+1)$$

$$(2,6) = \frac{1}{2}\sqrt{\frac{J-1}{2J+1}}\left[(b(J+1) - \beta)\right]$$

$$(3,5) = -\frac{1}{2}\sqrt{\frac{J-1}{2J+1}}\left[(b(J+1) - \beta)\right]$$

$$(3,6) = \frac{1}{2}qJ(J-1)$$

$$(2,4) = -(1,5)\ ;\ (3,4) = (1,6)\ ;\ (4,5) = -(1,2)\ ;\ (4,6) = (1,3)\ ;\ (5,6) = -(2,3)$$

TABLE 1c
The Hamiltonian Matrix Elements for NH_2^+ Considered as Linear: The Bending Number of Vibration Quantum $v_2 = 2$

$$(1,1)^2_{F_3} = E_v + B_v[(J+1)(J+2)-4] - D_v[(J+1)(J+2)-4]^2 - (J+2)\left[(a-a_0) - \frac{12a}{(J+1)(J+2)}\right] - \alpha\frac{J+2}{2J+1}\left[1 - \frac{12}{J(J+1)}\right] + 4g_{22}$$

$$(2,2)^2_{F_2} = E_v + B_v[J(J+1)-4] - D_v[J(J+1)-4]^2 - \left[(a-a_0) - \frac{12a}{J(J+1)}\right] + \alpha\left[1 - \frac{12}{J(J+1)}\right] + 4g_{22}$$

$$(3,3)^2_{F_1} = E_v + B_v[J(J-1)-4] - D_v[J(J-1)-4]^2 + (J-1)\left[(a-a_0) - \frac{12a}{J(J-1)}\right] - \alpha\frac{J-1}{2J+1}\left[1 - \frac{12}{J(J-1)}\right] + 4g_{22}$$

$$(4,4)^{-2}_{F_3} = (1,1)^2_{F_3} \; ; \; (5,5)^{-2}_{F_2} = (2,2)^2_{F_2} \; ; \; (6,6)^{-2}_{F_1} = (3,3)^2_{F_1}$$

$$(7,7)^0_{F_3} = E_v + B_v[(J+1)(J+2)] - D_v[(J+1)(J+2)]^2 - (a-a_0)(J+2) - \alpha\frac{J+2}{2J+1}$$

$$(8,8)^0_{F_2} = E_v + B_v[J(J+1)] - D_v[J(J+1)]^2 - (a-a_0) + \alpha$$

$$(9,9)^0_{F_1} = E_v + B_v[J(J-1)] - D_v[J(J-1)]^2 + (a-a_0)(J-1) - \alpha\frac{J-1}{2J+1}$$

$$(1,2) = -\frac{6}{J+1}\sqrt{\frac{(J-1)(J+3)}{J(2J+1)}}(aJ+\alpha) \qquad (1,8) = \frac{1}{2}\sqrt{\frac{(J+2)(J+3)}{(J+1)(2J+1)}}(bJ+\beta)$$

$$(1,3) = 3\alpha\frac{\sqrt{(J-1)(J-2)(J+2)(J+3)}}{(2J+1)\sqrt{J(J+1)}} \qquad (1,9) = \frac{1}{2}\beta\frac{\sqrt{(J+2)(J+3)}}{2J+1}$$

$$(1,7) = \frac{1}{\sqrt{2}}q\{J(J+1)(J+2)(J+3)\}^{1/2} \qquad (2,3) = -\frac{6}{J}\sqrt{\frac{(J-2)(J+2)}{(J+1)(2J+1)}}[a(J+1)-\alpha]$$

$$(2,7) = -\frac{1}{2}\sqrt{\frac{(J-1)(J+2)}{(J+1)(2J+1)}}(bJ+\beta) \qquad (3,8) = -\frac{1}{2}\sqrt{\frac{(J-1)(J-2)}{J(2J+1)}}(b(J+1)-\beta)$$

$$(2,8) = \frac{1}{\sqrt{2}}q\{(J-1)J(J+1)(J+2)\}^{1/2} \qquad (3,9) = \frac{1}{\sqrt{2}}q\{(J-2)(J-1)J(J+1)\}^{1/2}$$

$$(2,9) = \frac{1}{2}\sqrt{\frac{(J-1)(J+2)}{J(2J+1)}}(b(J+1)-\beta) \qquad (7,9) = 3\alpha\frac{\sqrt{J(J+1)}}{2J+1}$$

$$(3,7) = \frac{1}{2}\beta\frac{\sqrt{(J-1)(J-2)}}{2J+1} \qquad (4,5) = -(1,2) \; ; \; (5,6) = -(2,3) \; ;$$

$$(4,8) = -(1,8) \; ; \; (5,7) = -(2,7) \; ; \; (5,8) = (1,8) \; ; \; (5,9) = -(2,9) \; ; (6,8) = -(3,8) \; ;$$

$$(6,9) = (3,9) \; ; \; (4,6) = (1,3) \; ; \; (4,7) = (1,7) \; ; \; (4,9) = (1,9) \; ; \; (6,7) = (3,7)$$

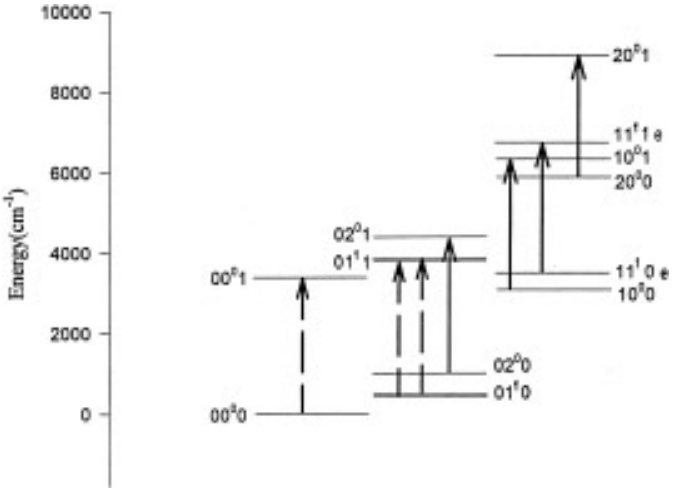

FIG. 3. Observed vibrational transitions of NH_2^+. Results of Okumura *et al.* (*13*) are shown with dashed lines.

diagram (*23*) indicates that if the bending potential is harmonic, the ν_2 value in the linear model is half of that of the bent model. Because of the highly anharmonic nature of the potential, however, the *ab initio* calculation of Jensen *et al.* (*7*) gave 313 cm^{-1} for the former and 922 cm^{-1} for the latter.

During the observation of the ν_3 fundamental band by Okumura *et al.* (*13*), NH_2^+ was considered as an asymmetric-top system. It is therefore of interest to establish the correspondence between the quantum numbers labeling the rotational levels of NH_2^+ as an asymmetric top (N, K_a, K_c) and those used for linear notation (N, ℓ_2, e, f). To this end, one must take into account the symmetry behavior of the two sets of wavefunctions associated with these quantum numbers when the parity operation is applied (*31*, *32*). For a vibronic state with (−) parity which applies to NH_2^+, the following equivalences are obtained:

Bent	Linear	
N	N	
K_a	ℓ_2	[1]
$(N + K_c)_{\text{even}}$	f	
$(N + K_c)_{\text{odd}}$	e	

The e and f correspondence is the opposite for a vibronic state with (+) parity.

Because NH_2^+ in its ground electronic state has two unpaired electrons, with a total electron spin $S = 1$, each rotational level splits into three components F_1 ($J = N + 1$), F_2 ($J = N$), and F_3 ($J = N - 1$). During the present work, the major observed transitions are the allowed ones $F_1 \leftarrow F_1$, $F_2 \leftarrow F_2$, and $F_3 \leftarrow F_3$, leading to the appearance of a triplet line structure, as shown in Fig. 2. These structures represent a fingerprint for the assignment although sometimes it was not easy to recognize. In fact, the line splitting can be as large as 0.7 cm^{-1} for low N values.

Another indication we used during the spectral assignment is the intensity alternation of 3:1. According to the Pauli principle and the $^3\Sigma_g^-$ ($^3B_1$) symmetry of the ground electronic state, the stronger lines correspond to transitions starting from even N'' levels for $\ell = 0$ and even N'' e sublevels and odd N'' f sublevels for $\ell = 1$. One recovers, of course, the rules observed with an asymmetric-top labeling (*13*), when the relations [1] are used.

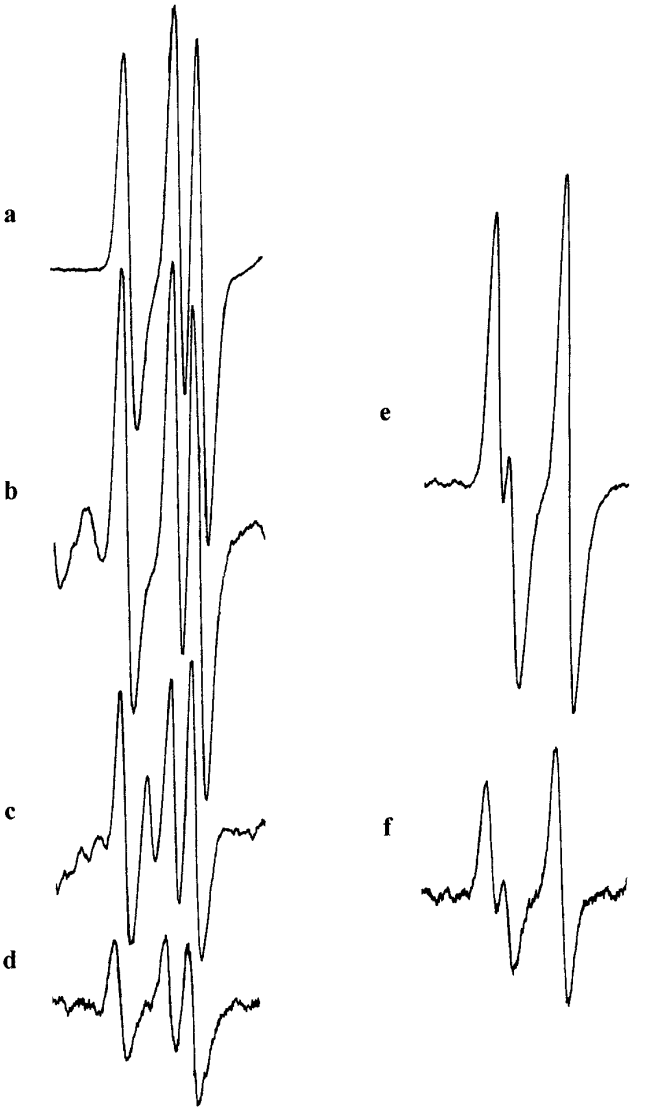

FIG. 4. Characteristic rotational fine structure of the observed bands of the NH_2^+ ion. Parts (a) to (d) are the $F_3 \leftarrow F_3$, $F_2 \leftarrow F_2$, and $F_1 \leftarrow F_1$ components of the $R(4)$ lines for the observed bands with $\ell_2 = 0$ ($\nu_3 \leftarrow 0$ (a), $\nu_1 + \nu_3 \leftarrow \nu_1$ (b), $2\nu_1 + \nu_3 \leftarrow 2\nu_1$ (c), $2\nu_2 + \nu_3 \leftarrow 2\nu_2$ (d)). Parts (e) and (f) are the $F_2 \leftarrow F_2$, $F_3 \leftarrow F_3$, and $F_1 \leftarrow F_1$ components of the P_e (4) lines of the observed bands with $\ell_2 = -1$ ($\nu_2 + \nu_3 \leftarrow \nu_2$ (e) and $\nu_1 + \nu_2 + \nu_3 \leftarrow \nu_1 + \nu_2$ (f)). In both cases the rotational fine structure spreads over 0.1 cm^{-1}.

TABLE 2
Molecular Constants (in cm^{-1}) of the Observed Bands of the NH_2^+ Ion

	00^01-00^00	$01^{\pm 1}1-01^{\pm 1}0$	02^01-02^00	10^01-10^00	$11^{-1}1-11^{-1}0$	20^01-20^00
ν_0	3359.9358(12)	3344.9292(11)	3331.210(19)	3226.03691(88)	3211.3491(22)	3081.5505(11)
B_v'	7.785627(79)	7.891603(96)	7.9021(20)	7.635036(57)	7.73196(16)	7.485985(81)
$D_v' x10^4$	2.8486(58)	2.8807(99)	29.51(48)	2.7043(44)	2.779(25)	2.7495(83)
q_e'	-	0.31292(15)	0.31292[a]	-	0.31292[a]	-
$q_N' x10^4$	-	-1.008(16)	-1.008[a]	-	-1.008[a]	-
$a' - a_0'$	-0.01149(40)	-0.01293(78)	-0.0128(11)	-0.01257(34)	-0.01293[a]	-0.01313(52)
a_0'	-	0.00707(79)	-	-	0.00707[a]	-
α'	0.6854(10)	0.6731(11)	0.6731[a]	0.6843(17)	0.6731[a]	0.6816(79)
B_v''	7.958759(74)	8.05604(11)	8.04649(34)	7.809987(59)	7.899835(82)	7.662887(74)
$D_v'' x10^4$	2.8420(59)	2.913(14)	23.219(64)	2.6944(54)	2.700(12)	2.7805(91)
q_e''	-	0.31581(16)	0.31581[a]	-	0.31581[a]	-
$q_N'' x10^4$	-	-1.026(23)	-1.026[a]	-	-1.026[a]	-
$a'' - a_0''$	-0.01182(39)	-0.01337(53)	-0.0129(11)	-0.01279(34)	-0.01337[a]	-0.01335(53)
a_0''	-	0.00570(57)	-	-	0.00570[a]	-
α''	0.69003(84)	0.67521(89)	0.67521[a]	0.6885(17)	0.67521[a]	0.6847(79)
RMS error	0.0044	0.0058	0.0057	0.0030	0.0024	0.0028
N data	84	155	21	74	39	58

All figures in parentheses are 1σ.

[a] Fixed to the $01^{\pm 1}1-01^{\pm 1}0$ transition value.

The presence in the spectra of a large number of absorption lines of HN_2^+ (*21*) sometimes complicated the NH_2^+ lines assignment. For some of these cases, the difference in their linewidths was helpful to discriminate between the two species.

In all, we were able to assign four new hot bands of the NH_2^+ ion. The corresponding vibrational transitions are shown in Fig. 3. The vibrational assignment of these bands was straightforward. First, it was observed that the rotational fine structure was characteristic for a given ℓ_2 value, as illustrated in Fig. 4 for $\ell_2 = 0$ and $\ell_2 = 1$. This gave us a good indication for the ν_2 assignment. Second, the calculated vibrational and rotational anharmonicity corrections, discussed in Section IV, take the typical values of a light triatomic molecule. Finally, we noticed that the transition scheme observed for NH_2^+, and given in Fig. 3, is analogous to a part of the observed case of the HN_2^+ ion produced in the same discharge (*21*), if the comparison is restricted to the lowest excited vibrational levels.

IV. ANALYSIS

To describe the ℓ-type doubling effect characterizing the degeneracy of the ν_2 vibration on one hand, and the splitting due to the electronic spin of NH_2^+ on the other, one must use an appropriate Hamiltonian model. The ℓ-type doubling effect as well as the Hamiltonian model necessary to build the corresponding matrix elements are well known (Ref. (*33*) and references therein). In order to analyze our spectrum, we need the expressions describing the coupling of the total electron spin S to the rotational angular momentum N for a linear triatomic system in an excited degenerate bending vibrational mode. To this end, we have used the Hamiltonian of Ref. (*13*), which is based on the original work of Van Vleck (*24*), and the correlation relations between asymmetric-top and linear molecule parameters presented in the same reference.

The Hamiltonian matrix elements for NH_2^+ are given by straightforward calculations, and the results for $v_2 = 0$, 1, 2 are given in Tables 1a, 1b, and 1c, respectively. Since the corresponding Hamiltonian matrices are symmetric, only the upper triangle elements are shown in these tables.

In these tables, E_v, B_v, D_v, and q are the vibrational term value, the rotational constant, the centrifugal distortion constant, and the ℓ-type doubling constant, respectively. If higher-order anharmonicity corrections are neglected, we have

TABLE 3

Assignment, Wavenumbers (in cm^{-1}), and Residuals (O − C in $cm^{-1} \times 10^4$) of the Observed Transitions of NH_2^+ in the Region between 3500 and 2900 cm^{-1}

Upper Level						Lower Level								Upper Level						Lower Level							
v_1	v_2	l_2	v_3	J	N	v_1	v_2	l_2	v_3	J	N	ν_{obs}	O-C	v_1	v_2	l_2	v_3	J	N	v_1	v_2	l_2	v_3	J	N	ν_{obs}	O-C
0	0	0	1	10	11	0	0	0	0	9	10	3510.6766*	106	0	0	0	1	6	7	0	0	0	0	5	6	3461.2972	4
0	0	0	1	12	11	0	0	0	0	11	10	3510.6478	68	0	0	0	1	7	7	0	0	0	0	6	6	3461.2643	-19
0	0	0	1	11	11	0	0	0	0	10	10	3510.6478	21	0	0	0	1	8	7	0	0	0	0	7	6	3461.2527	-32
0	1	1	1	11	12	0	1	1	0	10	11	3507.6366	-91	0	1	-1	1	6	7	0	1	-1	0	5	6	3450.3549	-122
0	1	1	1	12	12	0	1	1	0	11	11	3507.6366	30	0	1	-1	1	7	7	0	1	-1	0	6	6	3450.3549	-49
0	1	1	1	13	12	0	1	1	0	12	11	3507.5940*	-281	0	1	-1	1	8	7	0	1	-1	0	7	6	3450.3202	-73
0	1	-1	1	10	11	0	1	-1	0	9	10	3502.1696	-68	0	0	0	1	5	6	0	0	0	0	4	5	3447.9578	30
0	1	-1	1	11	11	0	1	-1	0	10	10	3502.1696	54	0	0	0	1	6	6	0	0	0	0	5	5	3447.9205	27
0	1	-1	1	12	11	0	1	-1	0	11	10	3502.1490	-16	0	0	0	1	7	6	0	0	0	0	6	5	3447.9043	-4
0	0	0	1	9	10	0	0	0	0	8	9	3498.9384	-3	0	1	1	1	6	7	0	1	1	0	5	6	3446.2404	-26
0	0	0	1	10	10	0	0	0	0	9	9	3498.9090	-78	0	1	1	1	7	7	0	1	1	0	6	6	3446.2404	47
0	0	0	1	11	10	0	0	0	0	10	9	3498.9090	-22	0	1	1	1	8	7	0	1	1	0	7	6	3446.2051	17
0	0	0	1	8	9	0	0	0	0	7	8	3486.7974	9	0	1	-1	1	6	6	0	1	-1	0	5	5	3436.4321	31
0	0	0	1	9	9	0	0	0	0	8	8	3486.7651	-76	0	1	-1	1	5	6	0	1	-1	0	4	5	3436.4321	24
0	0	0	1	10	9	0	0	0	0	9	8	3486.7651	-7	0	1	-1	1	7	6	0	1	-1	0	6	5	3436.3852	12
0	1	1	1	9	10	0	1	1	0	8	9	3484.2215	10	0	0	0	1	4	5	0	0	0	0	3	4	3434.2331	25
0	1	1	1	10	10	0	1	1	0	9	9	3484.2055	-29	0	0	0	1	5	5	0	0	0	0	4	4	3434.1850	31
0	1	1	1	11	10	0	1	1	0	10	9	3484.1910	-13	0	0	0	1	6	5	0	0	0	0	5	4	3434.1635	-13
0	1	-1	1	8	9	0	1	-1	0	7	8	3477.0774	32	0	1	1	1	5	6	0	1	1	0	4	5	3432.8453	-16
0	1	-1	1	9	9	0	1	-1	0	8	8	3477.0661	36	0	1	1	1	6	6	0	1	1	0	5	5	3432.8453	-9
0	1	-1	1	10	9	0	1	-1	0	9	8	3477.0430	1	0	1	1	1	7	6	0	1	1	0	6	5	3432.8001	-13
0	0	0	1	7	8	0	0	0	0	6	7	3474.2493	26	0	1	-1	1	5	5	0	1	-1	0	4	4	3422.1255	-10
0	0	0	1	8	8	0	0	0	0	7	7	3474.2211	10	0	1	-1	1	4	5	0	1	-1	0	3	4	3422.1105	-7
0	0	0	1	9	8	0	0	0	0	8	7	3474.2126	8	0	1	-1	1	6	5	0	1	-1	0	5	4	3422.0592	9
0	1	1	1	8	9	0	1	1	0	7	8	3471.9464	116	0	0	0	1	3	4	0	0	0	0	2	3	3420.1444	49
0	1	1	1	9	9	0	1	1	0	8	8	3471.9338	106	0	0	0	1	4	4	0	0	0	0	3	3	3420.0704	51
0	1	1	1	10	9	0	1	1	0	9	8	3471.9119	83	0	0	0	1	5	4	0	0	0	0	4	3	3420.0425	7
0	1	-1	1	7	8	0	1	-1	0	6	7	3463.9213	37	0	1	1	1	5	5	0	1	1	0	4	4	3419.0916	-132
0	1	-1	1	8	8	0	1	-1	0	7	7	3463.9135	62	0	1	1	1	4	5	0	1	1	0	3	4	3419.0802	-93
0	1	-1	1	9	8	0	1	-1	0	8	7	3463.8838	12	0	1	1	1	6	5	0	1	1	0	5	4	3419.0287	-80
0	1	-1	1	4	4	0	1	-1	0	3	3	3407.4707	-16	0	1	1	1	1	2	0	1	1	0	0	1	3374.7513	9
0	1	-1	1	3	4	0	1	-1	0	2	3	3407.4189	70	0	0	0	1	0	1	0	0	0	0	1	0	3374.1772	-12
0	1	-1	1	5	4	0	1	-1	0	4	3	3407.3584	41	1	0	0	1	10	11	1	0	0	0	9	10	3373.3295	8
0	2	0	1	4	5	0	2	0	0	3	4	3407.0015	-39	1	0	0	1	11	11	1	0	0	0	10	10	3373.3047	-22
0	2	0	1	5	5	0	2	0	0	4	4	3406.9541	53	1	0	0	1	12	11	1	0	0	0	11	10	3373.3047	53
0	2	0	1	6	5	0	2	0	0	5	4	3406.9314	-14	1	0	0	1	8	9	1	0	0	0	7	8	3350.0979	-1
0	0	0	1	2	3	0	0	0	0	1	2	3405.7234	-18	1	0	0	1	9	9	1	0	0	0	8	8	3350.0654	-76
0	0	0	1	3	3	0	0	0	0	2	2	3405.5683	-68	1	0	0	1	10	9	1	0	0	0	9	8	3350.0654	20
0	0	0	1	4	3	0	0	0	0	3	2	3405.5262*	-137	0	1	-1	1	4	3	0	1	1	0	4	3	3346.8781	-8
0	1	1	1	4	4	0	1	1	0	3	3	3405.0271	-19	0	1	-1	1	3	3	0	1	1	0	3	3	3346.8404*	-357
0	1	1	1	3	4	0	1	1	0	2	3	3404.9680	-4	0	1	-1	1	2	3	0	1	1	0	2	3	3346.8289*	-500
0	1	1	1	5	4	0	1	1	0	4	3	3404.9090	-23	0	1	-1	1	0	1	0	1	1	0	1	1	3346.4310	-91
0	2	0	1	3	4	0	2	0	0	2	3	3392.6363	19	0	1	-1	1	3	2	0	1	1	0	3	2	3345.9901	13
0	2	0	1	4	4	0	2	0	0	3	3	3392.5544	30	0	1	-1	1	1	2	0	1	1	0	1	2	3345.9509*	-393
0	2	0	1	5	4	0	2	0	0	4	3	3392.5243	-48	0	1	-1	1	2	2	0	1	1	0	2	2	3345.9509*	-365
0	1	-1	1	3	3	0	1	-1	0	2	2	3392.5243	6	0	1	-1	1	2	1	0	1	1	0	1	1	3345.7924	-141
0	1	-1	1	2	3	0	1	-1	0	1	2	3392.2709*	-190	0	1	-1	1	2	1	0	1	1	0	2	1	3345.3978	75
0	1	-1	1	4	3	0	1	-1	0	3	2	3392.2709	18	0	1	-1	1	1	1	0	1	1	0	1	1	3345.3978	45
0	0	0	1	1	2	0	0	0	0	0	1	3391.4439	-50	0	1	-1	1	0	1	0	1	1	0	0	1	3345.3978	22
0	0	0	1	2	2	0	0	0	0	1	1	3390.7229	48	0	0	0	1	1	0	0	0	0	0	0	1	3345.3510	-45
0	1	1	1	3	3	0	1	1	0	2	2	3390.6785	48	0	1	1	1	0	1	0	1	-1	0	1	1	3345.1861	2
0	0	0	1	3	2	0	0	0	0	2	1	3390.6596	21	0	1	-1	1	1	1	0	1	1	0	2	1	3344.9743	-27
0	1	1	1	2	3	0	1	1	0	1	2	3390.4425	32	0	1	1	1	2	1	0	1	-1	0	1	1	3344.5586	61
0	1	1	1	4	3	0	1	1	0	3	2	3390.4233	36	0	1	-1	1	1	1	0	1	1	0	0	1	3344.3457	-30
0	2	0	1	2	3	0	2	0	0	1	2	3377.8579	-27	0	0	0	1	1	0	0	0	0	0	2	1	3344.1482*	-137
0	2	0	1	3	3	0	2	0	0	2	2	3377.7051	40	0	1	1	1	2	1	0	1	-1	0	2	1	3344.1482	142
0	2	0	1	4	3	0	2	0	0	3	2	3377.6642	-13	0	1	1	1	0	1	0	1	-1	0	0	1	3344.1482	93
0	1	-1	1	2	2	0	1	-1	0	1	1	3377.6642	52	0	1	1	1	1	1	0	1	-1	0	1	1	3344.1482	66
0	1	-1	1	3	2	0	1	-1	0	2	1	3376.7646	-38	0	1	1	1	1	1	0	1	-1	0	2	1	3343.7329	98
0	1	1	1	2	2	0	1	1	0	1	1	3376.4165	11	0	0	0	1	1	0	0	0	0	0	1	1	3343.2925	-48
0	0	0	1	1	1	0	0	0	0	1	0	3376.2237	6	0	1	1	1	1	1	0	1	-1	0	0	1	3343.0983	37
0	1	1	1	3	2	0	1	1	0	2	1	3375.5250	-6	0	1	1	1	3	2	0	1	-1	0	3	2	3342.2503*	265
0	0	0	1	2	1	0	0	0	0	1	0	3375.3521*	-124	0	1	1	1	1	2	0	1	-1	0	1	2	3342.2221	-79

Note . Transitions rejected from the fit are indicated by an asterisk.

TABLE 3—*Continued*

Upper Level						Lower Level							
v_1	v_2	ℓ_2	v_3	J	N	v_1	v_2	ℓ_2	v_3	J	N	ν_{obs}	O-C
0	1	1	1	2	2	0	1	-1	0	2	2	3342.2221	-31
1	0	0	1	7	8	1	0	0	0	6	7	3337.8657	-9
1	0	0	1	8	8	1	0	0	0	7	7	3337.8386	-3
1	0	0	1	9	8	1	0	0	0	8	7	3337.8262	-18
0	0	0	1	2	1	0	0	0	0	3	2	3327.8320	-2
0	0	0	1	1	1	0	0	0	0	2	2	3327.7595	8
0	0	0	1	0	1	0	0	0	0	1	2	3327.0590	88
1	0	0	1	6	7	1	0	0	0	5	6	3325.2317	-22
1	0	0	1	7	7	1	0	0	0	6	6	3325.2014	-9
1	0	0	1	8	7	1	0	0	0	7	6	3325.1892	-3
1	1	-1	1	6	7	1	1	-1	0	5	6	3314.4024	-35
1	1	-1	1	7	7	1	1	-1	0	6	6	3314.4024	39
1	1	-1	1	8	7	1	1	-1	0	7	6	3314.3656	-6
0	1	1	1	0	1	0	1	1	0	1	2	3314.1310	-75
0	1	-1	1	0	1	0	1	-1	0	1	2	3312.8856	104
1	0	0	1	5	6	1	0	0	0	4	5	3312.2106	28
1	0	0	1	6	6	1	0	0	0	5	5	3312.1718	19
1	0	0	1	7	6	1	0	0	0	6	5	3312.1550	5
0	1	-1	1	2	1	0	1	-1	0	3	2	3312.0923	38
0	0	0	1	3	2	0	0	0	0	4	3	3311.2228	31
0	1	-1	1	1	1	0	1	-1	0	2	2	3311.2013	-18
0	0	0	1	2	2	0	0	0	0	3	3	3311.1722	20
0	0	0	1	1	2	0	0	0	0	2	3	3311.0335	-29
1	1	-1	1	6	6	1	1	-1	0	5	5	3300.8335	9
1	1	-1	1	5	6	1	1	-1	0	4	5	3300.8335	2
1	1	-1	1	7	6	1	1	-1	0	6	5	3300.7867	-9
1	0	0	1	4	5	1	0	0	0	3	4	3298.8002	25
1	0	0	1	5	5	1	0	0	0	4	4	3298.7499	17
1	0	0	1	6	5	1	0	0	0	5	4	3298.7291	1
0	1	1	1	3	2	0	1	1	0	4	3	3296.8320	-16
0	1	1	1	1	2	0	1	1	0	2	3	3296.8131	-59
0	1	1	1	2	2	0	1	1	0	3	3	3296.5757	-19
0	1	-1	1	3	2	0	1	-1	0	4	3	3294.9525*	201
0	1	-1	1	3	4	0	1	-1	0	4	5	3259.8073*	203
0	1	-1	1	4	4	0	1	-1	0	5	5	3259.7870*	198
0	0	0	1	6	5	0	0	0	0	7	6	3259.5044	-25
0	0	0	1	5	5	0	0	0	0	6	6	3259.4767	-1
0	0	0	1	4	5	0	0	0	0	5	6	3259.4491	-24
1	1	-1	1	3	3	1	1	-1	0	2	2	3257.9705	12
1	1	-1	1	2	3	1	1	-1	0	1	2	3257.7290	-62
1	1	-1	1	4	3	1	1	-1	0	3	2	3257.7166	19
1	0	0	1	1	2	1	0	0	0	0	1	3256.9435	-5
1	0	0	1	2	2	1	0	0	0	1	1	3256.2167	26
1	0	0	1	3	2	1	0	0	0	2	1	3256.1508	-10
0	2	0	1	5	4	0	2	0	0	6	5	3247.5112*	517
0	2	0	1	4	4	0	2	0	0	5	5	3247.4766*	402
0	2	0	1	3	4	0	2	0	0	4	5	3247.4370*	496
0	1	1	1	6	5	0	1	1	0	7	6	3245.6592	-15
0	1	1	1	4	5	0	1	1	0	5	6	3245.6072	-25
0	1	1	1	5	5	0	1	1	0	6	6	3245.6072	2
0	1	-1	1	6	5	0	1	-1	0	7	6	3241.8688	-55
0	1	-1	1	4	5	0	1	-1	0	5	6	3241.8207	-24
0	1	-1	1	5	5	0	1	-1	0	6	6	3241.8207	3
0	0	0	1	7	6	0	0	0	0	8	7	3241.6576	40
0	0	0	1	6	6	0	0	0	0	7	7	3241.6310	55
0	0	0	1	5	6	0	0	0	0	6	7	3241.6089	31
1	0	0	1	2	1	1	0	0	0	1	0	3241.1624	-13
0	2	0	1	6	5	0	2	0	0	7	6	3229.6714	34
0	2	0	1	5	5	0	2	0	0	6	6	3229.6443	-23
0	2	0	1	4	5	0	2	0	0	5	6	3229.6105	-11
0	1	1	1	7	6	0	1	1	0	8	7	3228.0262	-11
0	1	1	1	5	6	0	1	1	0	6	7	3227.9838	41
0	1	1	1	6	6	0	1	1	0	7	7	3227.9838	-9
0	1	-1	1	7	6	0	1	-1	0	8	7	3223.6296	15
0	1	-1	1	5	6	0	1	-1	0	6	7	3223.5846	42
0	1	-1	1	6	6	0	1	-1	0	7	7	3223.5846	-9

Upper Level						Lower Level							
v_1	v_2	ℓ_2	v_3	J	N	v_1	v_2	ℓ_2	v_3	J	N	ν_{obs}	O-C
0	1	-1	1	1	2	0	1	-1	0	2	3	3294.9355*	189
0	1	-1	1	2	2	0	1	-1	0	3	3	3294.6709	-49
0	0	0	1	4	3	0	0	0	0	5	4	3294.2861	-86
0	0	0	1	3	3	0	0	0	0	4	4	3294.2497	-62
0	0	0	1	2	3	0	0	0	0	3	4	3294.1893	-66
1	1	-1	1	5	5	1	1	-1	0	4	4	3286.8854	-1
1	1	-1	1	4	5	1	1	-1	0	3	4	3286.8697	-5
1	1	-1	1	6	5	1	1	-1	0	5	4	3286.8162	-11
1	0	0	1	3	4	1	0	0	0	2	3	3285.0189	3
1	0	0	1	4	4	1	0	0	0	3	3	3284.9459	19
1	0	0	1	5	4	1	0	0	0	4	3	3284.9198	14
0	1	1	1	4	3	0	1	1	0	5	4	3280.0631	2
0	1	1	1	2	3	0	1	1	0	3	4	3280.0054	-10
0	1	1	1	3	3	0	1	1	0	4	4	3279.9383	-17
0	1	-1	1	4	3	0	1	-1	0	5	4	3277.5298	17
0	1	-1	1	2	3	0	1	-1	0	3	4	3277.4699	-12
0	1	-1	1	3	3	0	1	-1	0	4	4	3277.3982	-67
0	0	0	1	5	4	0	0	0	0	6	5	3277.0603	45
0	0	0	1	4	4	0	0	0	0	5	5	3277.0289	64
0	0	0	1	3	4	0	0	0	0	4	5	3276.9910	44
1	1	-1	1	4	4	1	1	-1	0	3	3	3272.5784	0
1	1	-1	1	3	4	1	1	-1	0	2	3	3272.5197	18
1	1	-1	1	5	4	1	1	-1	0	4	3	3272.4629	25
1	0	0	1	2	3	1	0	0	0	1	2	3270.9145	6
1	0	0	1	3	3	1	0	0	0	2	2	3270.7640	2
1	0	0	1	4	3	1	0	0	0	3	2	3270.7227	-39
0	2	0	1	4	3	0	2	0	0	5	4	3264.9337	17
0	2	0	1	3	3	0	2	0	0	4	4	3264.8968	-63
0	2	0	1	2	3	0	2	0	0	3	4	3264.8324	47
0	1	1	1	5	4	0	1	1	0	6	5	3263.0053	-15
0	1	1	1	3	4	0	1	1	0	4	5	3262.9502	-12
0	1	1	1	4	4	0	1	1	0	5	5	3262.9281	-33
0	1	-1	1	5	4	0	1	-1	0	6	5	3259.8600*	173
0	0	0	1	8	7	0	0	0	0	9	8	3223.4956	-67
0	0	0	1	7	7	0	0	0	0	8	8	3223.4741	-12
0	0	0	1	6	7	0	0	0	0	7	8	3223.4546	-42
0	1	1	1	8	7	0	1	1	0	9	8	3210.1111	1
0	1	1	1	7	7	0	1	1	0	8	8	3210.0726	-23
0	1	1	1	6	7	0	1	1	0	7	8	3210.0726	68
0	0	0	1	9	8	0	0	0	0	10	9	3205.0585	-7
0	0	0	1	7	8	0	0	0	0	8	9	3205.0387*	203
0	0	0	1	8	8	0	0	0	0	9	9	3205.0387	56
2	0	0	1	8	9	2	0	0	0	7	8	3202.7949	-12
2	0	0	1	9	9	2	0	0	0	8	8	3202.7705	-18
2	0	0	1	10	9	2	0	0	0	9	8	3202.7600	-8
1	0	0	1	2	1	1	0	0	0	3	2	3194.5258	10
1	0	0	1	1	1	1	0	0	0	2	2	3194.4506	-7
1	0	0	1	0	1	1	0	0	0	1	2	3193.7392	-26
0	1	1	1	9	8	0	1	1	0	10	9	3191.9128	-45
0	1	1	1	8	8	0	1	1	0	9	9	3191.8768	-83
0	1	1	1	7	8	0	1	1	0	8	9	3191.8768	32
2	0	0	1	7	8	2	0	0	0	6	7	3190.8902	7
2	0	0	1	8	8	2	0	0	0	7	7	3190.8659	28
2	0	0	1	9	8	2	0	0	0	8	7	3190.8530	28
0	0	0	1	9	9	0	0	0	0	10	10	3186.3344*	291
0	0	0	1	10	9	0	0	0	0	11	10	3186.3344	34
0	0	0	1	8	9	0	0	0	0	9	10	3186.2880	-39
2	0	0	1	6	7	2	0	0	0	5	6	3178.5796	0
2	0	0	1	7	7	2	0	0	0	6	6	3178.5488	-6
2	0	0	1	8	7	2	0	0	0	7	6	3178.5337	-9
1	0	0	1	3	2	1	0	0	0	4	3	3178.1994	-20
1	0	0	1	2	2	1	0	0	0	3	3	3178.1465	-55
1	0	0	1	1	2	1	0	0	0	2	3	3178.0193	24
2	0	0	1	5	6	2	0	0	0	4	5	3165.8751	13
2	0	0	1	6	6	2	0	0	0	5	5	3165.8383	11
2	0	0	1	7	6	2	0	0	0	6	5	3165.8195	-4

TABLE 3—*Continued*

Upper Level						Lower Level							
v_1	v_2	ℓ_2	v_3	J	N	v_1	v_2	ℓ_2	v_3	J	N	ν_{obs}	O-C
1	0	0	1	4	3	1	0	0	0	5	4	3161.5609	2
1	0	0	1	3	3	1	0	0	0	4	4	3161.5239	19
1	0	0	1	2	3	1	0	0	0	3	4	3161.4599	-9
2	0	0	1	4	5	2	0	0	0	3	4	3152.7800	-8
2	0	0	1	5	5	2	0	0	0	4	4	3152.7330	2
2	0	0	1	6	5	2	0	0	0	5	4	3152.7110	-6
1	1	-1	1	4	3	1	1	-1	0	5	4	3145.1543	9
1	1	-1	1	2	3	1	1	-1	0	3	4	3145.0970	5
1	1	-1	1	3	3	1	1	-1	0	4	4	3145.0299	-3
1	0	0	1	5	4	1	0	0	0	6	5	3144.6020	10
1	0	0	1	4	4	1	0	0	0	5	5	3144.5707	28
1	0	0	1	3	4	1	0	0	0	4	5	3144.5325	17
2	0	0	1	3	4	2	0	0	0	2	3	3139.3135	-18
2	0	0	1	4	4	2	0	0	0	3	3	3139.2424	1
2	0	0	1	5	4	2	0	0	0	4	3	3139.2154	6
1	1	-1	1	5	4	1	1	-1	0	6	5	3127.7460	9
1	1	-1	1	3	4	1	1	-1	0	4	5	3127.6916	21
1	1	-1	1	4	4	1	1	-1	0	5	5	3127.6675	-21
1	0	0	1	6	5	1	0	0	0	7	6	3127.3205	-53
1	0	0	1	5	5	1	0	0	0	6	6	3127.2939	-21
1	0	0	1	4	5	1	0	0	0	5	6	3127.2670	-27
2	0	0	1	2	3	2	0	0	0	1	2	3125.5210	9
2	0	0	1	3	3	2	0	0	0	2	2	3125.3721	0
2	0	0	1	4	3	2	0	0	0	3	2	3125.3331	-1
2	0	0	1	1	2	2	0	0	0	0	1	3111.8107*	-427
2	0	0	1	2	2	2	0	0	0	1	1	3111.1250	-36
2	0	0	1	3	2	2	0	0	0	2	1	3111.0652	5
1	1	-1	1	6	5	1	1	-1	0	7	6	3110.0410	-7
1	1	-1	1	4	5	1	1	-1	0	5	6	3109.9880	-25
1	1	-1	1	5	5	1	1	-1	0	6	6	3109.9880	2
1	0	0	1	7	6	1	0	0	0	8	7	3109.7434	31
1	0	0	1	6	6	1	0	0	0	7	7	3109.7183	56
1	0	0	1	5	6	1	0	0	0	6	7	3109.6948	29
2	0	0	1	5	6	2	0	0	0	4	5	3096.3775	-17
1	1	-1	1	7	6	1	1	-1	0	8	7	3092.0472	8
1	1	-1	1	6	6	1	1	-1	0	7	7	3092.0016	-22
1	1	-1	1	5	6	1	1	-1	0	6	7	3092.0016	28
1	0	0	1	8	7	1	0	0	0	9	8	3091.8516	11
1	0	0	1	7	7	1	0	0	0	8	8	3091.8259	18
1	0	0	1	6	7	1	0	0	0	7	8	3091.8093	26
1	0	0	1	9	8	1	0	0	0	10	9	3073.6589	-34
1	0	0	1	8	8	1	0	0	0	9	9	3073.6348	-20
1	0	0	1	7	8	1	0	0	0	8	9	3073.6190	-24
2	0	0	1	2	1	2	0	0	0	3	2	3050.6209	-23
2	0	0	1	1	1	2	0	0	0	2	2	3050.5503	-5
2	0	0	1	0	1	2	0	0	0	1	2	3049.8653*	242
2	0	0	1	3	2	2	0	0	0	4	3	3034.5915	45
2	0	0	1	2	2	2	0	0	0	3	3	3034.5406	20
2	0	0	1	1	2	2	0	0	0	2	3	3034.4079	61
2	0	0	1	4	3	2	0	0	0	5	4	3018.2341	35
2	0	0	1	3	3	2	0	0	0	4	4	3018.1948	19
2	0	0	1	2	3	2	0	0	0	3	4	3018.1285	-11
2	0	0	1	5	4	2	0	0	0	6	5	3001.5448	-78
2	0	0	1	4	4	2	0	0	0	5	5	3001.5180	-26
2	0	0	1	3	4	2	0	0	0	4	5	3001.4799	-14
2	0	0	1	6	5	2	0	0	0	7	6	2984.5573	0
2	0	0	1	5	5	2	0	0	0	6	6	2984.5275	-10
2	0	0	1	4	5	2	0	0	0	5	6	2984.4990	-9
2	0	0	1	7	6	2	0	0	0	8	7	2967.2503*	264
2	0	0	1	6	6	2	0	0	0	7	7	2967.2503	-3
2	0	0	1	5	6	2	0	0	0	6	7	2967.2029	20
2	0	0	1	8	7	2	0	0	0	9	8	2949.6173*	-218
2	0	0	1	7	7	2	0	0	0	8	8	2949.6173	36
2	0	0	1	6	7	2	0	0	0	7	8	2949.5915	-25

Note. The *e* and *f* levels are denoted by $\ell_2 = -1$ and $+1$, respectively.

$$E_v = \sum_t \omega_t\left(v_t + \frac{d_t}{2}\right) + \sum_{t\leqslant t'} x_{tt'}\left(v_t + \frac{d_t}{2}\right)\left(v_{t'} + \frac{d_{t'}}{2}\right) + g_{22}\ell_2^2 + \sum_t y_t^{22}\left(v_t + \frac{d_t}{2}\right)\ell_2^2 + \sum_{t\leqslant t'\leqslant t''} y_{tt't''} \times \left(v_t + \frac{d_t}{2}\right)\left(v_{t'} + \frac{d_{t'}}{2}\right)\left(v_{t''} + \frac{d_{t''}}{2}\right), \quad [2]$$

$$B_v = B_e - \sum_t a_t\left(v_t + \frac{d_t}{2}\right), \quad [3]$$

$$q = q_e + q_N N(N+1), \quad [4]$$

where each of t, t', t'' takes values of 1–3, and $d_1 = 1$, $d_2 = 2$, $d_3 = 1$. The parameter q_e in Eq. [4] can be expressed as (*34*)

$$q_e = \frac{2B_e^2}{\omega_e}\left(1 + \frac{4\omega_2^2}{\omega_3^2 - \omega_2^2}\right). \quad [5]$$

The parameters α, β and a, a_0, b appearing in Tables 1a–1c are the spin–spin and the spin–rotation constants, respectively.

When it was possible, a block-diagonalization of the Hamiltonian matrices was performed by using Wang-type basis functions. Consequently, the levels were characterized by an *e* or *f* label, defined in such a way that the ℓ-type doubling parameter q is positive (*33*).

A least-squares fit of the new observed transitions as well as those assigned by Okumura *et al.* (*13*) was carried out. The resulting molecular parameters are listed in Table 2 and are discussed in the next section. During the fitting procedures, combination differences were used but they are not given in Table 3, where the rovibrational transitions are sorted by descending frequencies. Many of the lines with large residuals (O − C) are those overlapped with other lines or observed in regions lacking reference signals.

V. DISCUSSION

As shown in Table 3, the obtained root-mean-squares errors after the least-squares fits of the observed bands are

TABLE 4

Equilibrium Rotational Constant, Associated Vibrational Corrections, and Vibrational Parameters of NH_2^+ in the Ground Electronic State

Constant	Value (cm^{-1})
B_e	8.022966
α_1	0.148788
α_2	- 0.096785
α_3	0.173164
$\omega_3 + 2x_{33} + 13/4y_{333}$	3439.8
$x_{13} + 2y_{133}$	- 123.6
x_{23}	- 17.6
y_{113}	- 5.3
y_{123}	0.3
y_{223}	0.8

typically within the uncertainty of the measurements, i.e., 0.003 cm^{-1}. During these fits, the constants b and β were not included since they do not improve the final results. Their values were consequently held fixed to zero.

For the 02^01-02^00, and the 11^11-11^10 transitions the ℓ-type doubling, the spin–spin, and the spin–rotation constants were held fixed to the values of the 01^11-01^10 band. In fact, in spite of a careful search, we were not able to assign with enough confidence rovibrational lines associated with the $\ell_2 = 2$ subbands of the 021–020 transition and the f subband of the 111–110 transition. This might be due to a larger perturbation with other states or to the weak intensities of these lines. The anomalously large centrifugal distortion constant in the case of the 02^01-02^00 band is a consequence of the ℓ-type resonance which was not properly taken into account.

The characterization of the rotational structure of the ground, the ν_1, the ν_2, and the ν_3 vibrational states allowed us to determine the equilibrium rotational constant, B_e, as well as the α_t ($t = 1, 2, 3$) parameters. These parameters, presented in Table 4, were determined from Eq. [3] after we used the rotational constants of the given vibrational states, listed in Table 2. The other vibrational parameters also listed in Table 4 have been obtained from the expression of the term value E_v (Eq. [2]). The values of the anharmonicity parameters are typical of a light triatomic molecule, especially the sum $x_{13} + 2y_{133}$. The same comment holds for the value of the α_t constants, and made us quite confident in our vibrational assignments.

The equilibrium rotational constant $B_e = 8.022966$ cm^{-1} gives the equilibrium bond length $r_e = 1.021$ Å which compares with theoretical values of $r_e = 1.0338$ Å (*7*) and $r_e = 1.030$ Å (*8, 14*). This discrepancy, which is clearly larger than the uncertainties both for experimental and theoretical values, probably resulted from our simplistic model of the linear molecule which ignores the quasilinear nature of NH_2^+.

By using the q''_e parameter given in Table 2, and the B_e constant listed in Table 4, it was possible calculate the ω_2 value to be 439 cm^{-1}. This value is approximately half of the ω_2 value of 918 cm^{-1} predicted by Jensen *et al.* (*7*) and 845 cm^{-1} predicted by Barclay *et al.* (*8*). While the value is probably not accurate because it is based on the simple vibration–rotation theory using perturbation treatment, it is reasonable in view of our use of the linear molecule formalism as opposed to their asymmetric rotor model.

It is important to underline that the variational rovibrational calculations of Ref. (*14*), considering NH_2^+ as an asymmetric rotor, predicts the 01^10-00^00 with a weak intensity, and the pure rotational band 000–000 with a reasonable intensity. The last transition corresponds precisely to the 01^10-00^00 band when the linear molecule notations are used. Therefore, in order to obtain experimental information on the bending potential, it is essential to investigate the 400 cm^{-1} region to attempt the observation of the $\nu_2^1 \leftarrow 0$ band of the NH_2^+ ion.

Finally, as shown by Okumura *et al.* (*13*), it is important to point out that the molecular constants derived during the present work from a linear molecule Hamiltonian model can be transformed into the asymmetric rotor parameters. The results presented in the present paper for the 00^01-00^00, and the 01^11-01^10 bands are therefore directly related to the parameters given in Ref. (*13*).

VI. CONCLUSIONS

The observation of four new hot bands of the amidogen ion, NH_2^+, in the region of the ν_3 fundamental band was reported. For its extreme quasilinearity, we used rovibrational quantum numbers for a linear molecule instead of the asymmetric rotor quantum numbers. The matrix elements of an appropriate Hamiltonian model describing the rotational fine structure of the degenerate bending vibrational levels were derived and presented. The obtained vibrational and rotational molecular constants were given and discussed. The value of the ℓ-type doubling constant was used to estimate the ν_2 bending vibration frequency to be around 439 cm^{-1}.

A natural continuation of this work is therefore to search for the $\nu_2^1 \leftarrow 0$ fundamental band in this region, in order to characterize the bending potential of this important species.

ACKNOWLEDGMENTS

We thank C. M. Gabrys for his help in recording part of the spectrum, and P. Jensen and P. Rosmus for making their results available to us prior to publication. The authors are also grateful to J. T. Hougen for stimulating discussions, and to P. R. Bunker for his critical reading of the manuscript. T. R. Huet acknowledges the support of the F.N.R.S. (Belgium) for a position as Senior Research Assistant (1991–1993). This work was supported by NSF Grant PHY-90-22647.

REFERENCES

1. E. Herbst and W. Klemperer, *Astrophys. J.* **185,** 505–534 (1973).
2. S. S. Prasad and W. T. Huntress, Jr., *Astrophys. J. Suppl.* **43,** 1–35 (1980).
3. E. F. van Dishoeck and J. H. Black, *Astrophys. J. Suppl.* **62,** 109–145 (1986).
4. A. D. Walsh, *J. Chem. Soc.*, 2260–2266 (1953).
5. S. T. Lee and K. Morokuma, *J. Am. Chem. Soc.* **93,** 6863–6866 (1971).
6. S. D. Peyerimhoff and R. J. Buenker, *Chem. Phys.* **42,** 167–176 (1979).
7. P. Jensen, P. R. Bunker, and A. D. McLean, *Chem. Phys. Lett.* **141,** 53–57 (1987).
8. V. J. Barclay, I. P. Hamilton, and P. Jensen, *J. Chem. Phys.* **99,** 9709–9719 (1993).
9. G. Duxbury and C. Jungen, *Mol. Phys.* **63,** 981–998 (1988).
10. A. Alijah and G. Duxbury, *Mol. Phys.* **70,** 605–622 (1990).
11. M. Peric, R. J. Buenker, and S. D. Peyerimhoff, *Astrophys. Lett.* **24,** 69–73 (1984).
12. D. J. DeFrees and A. D. McLean, *J. Chem. Phys.* **82,** 333–341 (1985).
13. M. Okumura, B. D. Rehfuss, B. M. Dinelli, M. G. Bawendi, and T. Oka, *J. Chem. Phys.* **90,** 5918–5923 (1989).
14. G. Chambaud, W. Gabriel, T. Schmelz, P. Rosmus, A. Spielfiedel, and N. Feautrier, *Theor. Chim. Acta* **87,** 5–17 (1994).
15. P. R. Bunker, *in* ''Comparison of *Ab Initio* Quantum Chemistry with Experiment for Small Molecules: The State of the Art'' (R. J. Bartlett, Ed.), pp. 141–170, Reidel, Dordrecht, 1985.
16. H. F. Schaefer III, *Science* **231,** 1100–1107 (1986).
17. G. Herzberg and J. Schoosmith, *Nature* **183,** 1801–1802 (1959).
18. S. J. Dunlavey, J. M. Dyke, N. Jonathan, and A. Morris, *Mol. Phys.* **39,** 1121–1135 (1980).
19. G. Herzberg, *in* ''Molecular Ions: Spectroscopy, Structure, and Chemistry'' (T. A. Miller and V. E. Bondybey, Eds.), p. 5, North-Holland, Amsterdam, 1983.
20. S. T. Gibson, J. P. Greene, and J. Berkowitz, *J. Chem. Phys.* **83,** 4319–4328 (1985).
21. Y. Kabbadj, T. R. Huet, B. D. Rehfuss, C. M. Gabrys, and T. Oka, *J. Mol. Spectrosc.* **163,** 180–205 (1994).
22. T. R. Huet, Y. Kabbadj, C. M. Gabrys, and T. Oka, *J. Mol. Spectrosc.* **163,** 206–216 (1994).
23. J. W. C. Johns, *Can. J. Phys.* **45,** 2639–2650 (1967).
24. J. H. Van Vleck, *Rev. Mod. Phys.* **23,** 213–227 (1951).
25. M. W. Crofton, M.-F. Jagod, B. D. Rehfuss, W. A. Kreiner, and T. Oka, *J. Chem. Phys.* **88,** 666–678 (1987).
26. A. S. Pine, *J. Opt. Soc. Am.* **64,** 1683–1690 (1974).
27. M. G. Bawendi, B. D. Rehfuss, and T. Oka, *J. Chem. Phys.* **93,** 6200–6209 (1990).
28. C. S. Gudeman, M. H. Begemann, J. Pfaff, and R. J. Saykally, *Phys. Rev. Lett.* **50,** 727–731 (1983).
29. J. W. C. Johns, private communication.
30. A. S. Pine, MIT Lincoln Laboratory Report NSF/ASRA/DAR-78-24562 (1981).
31. J. M. Brown, J. T. Hougen, K. P. Huber, J. W. C. Johns, I. Kopp, H. Lefebvre-Brion, A. J. Merer, D. A. Ramsay, J. Rostas, and R. N. Zare, *J. Mol. Spectrosc.* **55,** 500–503 (1975).
32. P. R. Bunker, ''Molecular Symmetry and Spectroscopy,'' Academic Press, Orlando, (1979).
33. M. Herman, T. R. Huet, Y. Kabbadj, and J. Vander Auwera, *Mol. Phys.* **72,** 75–88 (1991).
34. G. Herzberg, ''The Spectra and Structures of Simple Free Radicals: An Introduction to Molecular Spectroscopy,'' Dover, New York, 1971.